

Electrostatic Interactions in the Formation of DNA Complexes with Cis- and Trans-Isomers of Azobenzene-Containing Surfactants in Solutions with Di- and Trivalent Metal Ions

Nina A. Kasyanenko, Irina A. Silanteva,* Pavel V. Gabrusenok, Svetlana Santer, and Andrei V. Komolkin



Cite This: *ACS Omega* 2023, 8, 14597–14609



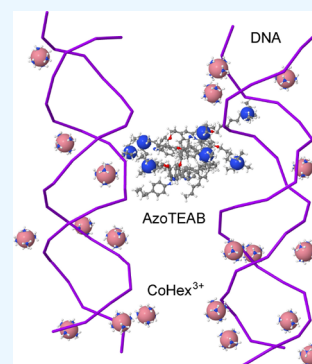
Read Online

ACCESS |

Metrics & More

Article Recommendations

ABSTRACT: The effect of the presence of divalent and trivalent metal ions in solutions upon DNA packaging induced by the photosensitive azobenzene-containing surfactant is considered. It has been shown that the addition of divalent and trivalent metal ions does not affect the DNA–surfactant interaction for both the cis- and the trans-isomers of the surfactant. At the same time, the ionic strength of the solution, which is provided by a certain concentration of the salt, has a huge impact. It affects the association of surfactant molecules with each other and their binding to DNA. It has been shown by computer simulation that cobalt hexamine is attracted to the N7 atom of guanine in the major groove of DNA and does not penetrate into grooves near the AT base pairs.



INTRODUCTION

DNA interaction with light-sensitive azobenzene-containing surfactants is rather well investigated and described in the literature. Nevertheless, interest in a comprehensive study of the properties of such systems has increased due to the prospects for their usage in new developments. The design and synthesis of different photoresponsive azobenzene-containing DNA materials, including nanoplasmonic systems, are now developed.^{1–9}

The azobenzene unit provides light control over the reversible switching between the planar hydrophobic trans-isomers and the nonplanar hydrophilic cis-form with a pronounced dipole moment.¹⁰ The length of the hydrophobic tail allows manipulation of the surfactant hydrophobicity and determines, for example, the size of the micelles and the CMC. However, the length of the tail does not fundamentally affect the nature of the surfactant interaction with DNA.^{11,12}

The reversible manipulation with DNA conformation realized with light was demonstrated using different azobenzene-containing surfactants.^{12–17} The azobenzene-containing surfactants in the trans-form cause a shrinkage of the DNA coil in a solution of low ionic strength, ultimately leading to a compact state. Surfactant molecules associate in aggregates on the polyelectrolyte DNA strand. The conformational transition of the swollen coil into a compact state is reversible. The DNA can again transform into a swollen random coil under UV irradiation, which converts the surfactant into a hydrophilic cis-form. Further irradiation with visible light leads to DNA compaction again due to the transition of surfactant

into a hydrophobic trans-form. This conformational transition should be distinguished from the phase transition with the formation of nanosized particles observed with an excess of surfactant in DNA solution.¹³

Interaction of cationic surfactants with negatively charged DNA and oligonucleotides in water solution depends greatly on the concentration of the supporting electrolyte (mainly NaCl).^{13,18–23} For example, the interaction does not occur at all at high salt concentration (1 M NaCl). The concentration of salt also affects the association of the surfactants in DNA-free solutions.^{24–28} The interaction of highly charged anionic DNA with positively charged compounds in solution essentially depends on the screening of the charges of the interacting components. In this regard for the dilute solutions of high-molecular DNA, the concept of the excluded volume of a macromolecule is used. This concept includes both the DNA polyelectrolyte swelling and the thermodynamic volume effects in terms of Flory's theory.²⁹ The excluded volume of the macromolecule is responsible for the absence of significant DNA packaging in solutions with a low concentration of polycations (low ratio of molar concentrations of ionogenic

Received: January 20, 2023

Accepted: April 4, 2023

Published: April 14, 2023



groups of polycation and DNA Z).³⁰ The emergence of nanosized interpolyelectrolyte complexes in dilute DNA solutions with polycations is observed at $Z > 1$.^{31,32} Note that the addition of small trivalent counterions of even very low concentrations (in terms of Z approximately at $Z < 0.01$) to a DNA solution would immediately lead to the formation of complexes with the decrease in the volume of the DNA molecular coil.^{33,34} In contrast to the DNA packaging induced by polycations, small multiply charged ions may cause the emergence of the nanosized DNA particles at their certain concentration, regardless of the charge ratio Z (i.e., regardless of the DNA concentration).³⁴ It should be noted that DNA packaging caused by cationic surfactants in aqueous solutions occurs at the charge ratio of about $Z = 1$, as it is usually observed in DNA solutions with polycations. The formation of nanosized structures in DNA–surfactant solutions is similar to that in DNA solutions with polycations, as it follows from the phase diagrams.^{13,30,34}

Cationic surfactants are amphiphilic molecules. Their binding to DNA decreases the charge density of the macromolecule and also transforms the environment around the double helix via the formation of a hydrophobic “coat” of the surfactant tails, which leads to a change in the DNA–solvent interaction. Note that even an extremely high NaCl concentration (more than 5 M) does not lead to DNA precipitation due to nonzero thermodynamic volume effects under such conditions.³⁵ On the contrary, for single-stranded DNA with hydrophobic bases exposed to the water, the ideal solvent (or theta solvent) is observed at 2 M NaCl. It is known that divalent metal ions shield the charge of the DNA molecule more effectively.^{36,37} Because they interact with the negatively charged oxygen atoms mainly through the water molecules,^{38,39} they cannot cause DNA condensation even at their high concentration in solution.^{40,41} In other words, for DNA condensation, it is necessary not only to have the effective shielding of negative charges, but also the reduction in the DNA hydrophilicity. Trivalent metal ions, as well as spermine and spermidine, induce DNA condensation in solutions.^{32,42–45} They provide a certain structuring of the DNA molecular coil in a solution due to their binding to sites that are remote along the chain; it helps to overcome the polyelectrolyte swelling.^{46–50}

There is an opinion that the binding of cobalt hexamine (CoHex³⁺) to DNA leads not only to DNA condensation,^{51–55} but also induces the B–A transition of the double helix.^{56,57} However, the study of the UV and circular dichroism spectra of DNA in the corresponding solutions does not confirm this for natural thymus DNA.³³ The assertion that CoHex³⁺ can bind not only to the oxygen of phosphate, but also to the N7 atom of guanine and some atoms of AT base pairs in the major groove of DNA, also exists.^{57,58} Note that any involvement of nitrogenous bases into binding leads to a change in the spectral properties of DNA and destabilizes its secondary structure, which is not observed when studying the binding of cobalt hexamine to DNA.^{33,46} However, such an interaction can be realized without double-stranded perturbation if cobalt is partially placed in the major or minor grooves of DNA without forming stable bonds with atomic groups of heterocycles. CoHex³⁺ cations are known to be able to enhance DNA condensation that is caused by the other agents.⁵⁹

In this work, we analyze the effect of the presence of divalent and trivalent metal ions in solutions upon DNA packaging induced by the surfactant. We chose a light-sensitive

azobenzene-containing surfactant that changes its conformation and, accordingly, its dipole moment under the action of UV and visible light. Azobenzene can exist in the trans- or cis-form. This property makes it possible to use azobenzene-based compounds for light-controlled DNA condensation and in various nanodevices.^{60,61} Surfactant interaction with DNA in solutions at different NaCl concentrations was previously studied in detail by our group^{13,24,62,63} and other researchers.^{19,64,65}

MATERIALS AND METHODS

High molecular calf thymus DNA (Sigma-Aldrich) with a molecular mass of 9×10^6 g/mol determined by viscometry

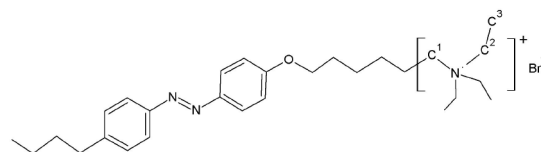


Figure 1. Structure of the azobenzene-containing surfactant.

and cationic azobenzene-containing surfactant (Figure 1) synthesized according to the synthesis scheme described in ref 66 were used. The VL-4.L UV lamp with a peak of emission at 355 nm and the diode light with a wavelength of 465 nm were used immediately before measurements for trans–cis and cis–trans isomerization of the azobenzene group in surfactant, respectively. The solutions in a quartz cuvette were irradiated by light sources placed at a distance of 2 cm from the samples. The salts MgCl₂, FeCl₃, LaCl₃, and Co(NH₃)₆Cl₃ from the Sigma-Aldrich Co. were also used.

Experimental Methods. Absorption spectra were registered with a spectrophotometer SF-56 (LOMO, Russia). Measurements were performed in a quartz cell with an optic path length of 1.0 cm.

We control the tertiary structure of the DNA molecule in solutions with surfactant by hydrodynamic methods. The model of a freely joined chain or the model of the wormlike (persistent) chain was usually applied to describe the conformation of DNA in solutions. For DNA samples with a molecular mass of more than $M = 2 \times 10^6$, both of these models are acceptable. The universal conformational parameters for these models are the mean square distance between the ends of the chain $(\overline{h^2})^{1/2}$, the contour (hydrodynamic) length L , and the molecular mass M . The length of the statistical segment (Kuhn segment) A and the persistent length p for the wormlike chain describes the bending (equilibrium) rigidity of the macromolecule.

In our experiment, a relative viscosity η_r of DNA solutions with and without surfactant and CoHex³⁺ was determined at 21 °C with a low gradient Zimm–Crothers-type rotation viscometer.⁶⁷ The velocity gradients did not exceed 3 s^{−1}, and therefore the study of the gradient dependence of viscosity is not necessary. The intrinsic viscosity of the DNA was obtained by the extrapolation of the dependence of reduced viscosity on the DNA concentration to the concentration $C = 0$:

$$[\eta] = \lim_{C \rightarrow 0} \lim_{g \rightarrow 0} \left(\frac{\eta_r - 1}{C} \right) \quad (1)$$

which is associated with the DNA conformational parameters by the equation:

Table 1. Simulated Systems

	I	II	III	IV	V
dsDNA 21 bp,	4	4	4	4	4
mM bp/l	0.125	0.116	0.115	0.116	0.115
trans-Azo, ions		42	42		
[trans-Azo], M		0.058	0.058		
cis-Azo, ions				42	42
[cis-Azo], M				0.058	0.058
CoHex ³⁺ , ions	56	42		42	
[CoHex ³⁺], M	0.083	0.058		0.058	
Na ⁺ , ions			126		126
[Na ⁺], M			0.173		0.173
H ₂ O, molecules	37447	40287	40455	40287	40455
box size, Å	70.98 × 128 × 128	70.98 × 134 × 134	70.98 × 134 × 134	70.98 × 134 × 134	70.98 × 134 × 134
simulation time, ns	55	86	92	82	145

$$[\eta] = \Phi \frac{(\overline{h^2})^{3/2}}{M} = \Phi \frac{(\overline{h_0^2})^{3/2}}{M} \alpha^3 = \Phi \frac{(LA)^{3/2}}{M} \alpha^3 \quad (2)$$

where Φ is a Flory parameter, M is the DNA molecular mass, and $(\overline{h^2})^{1/2}$ and $(\overline{h_0^2})^{1/2}$ are the mean-squared distances between the ends of the DNA chain in the real and the ideal solvents. Respectively, α is the coefficient of linear swelling, $\alpha = (\overline{h^2})^{1/2} / (\overline{h_0^2})^{1/2}$, L is the hydrodynamic length of the polymer chain, and A is the length of the Kuhn segment (chain rigidity parameter). For high molecular DNA samples, $A = 2p$. The optical anisotropy of DNA was determined with the flow birefringence method.^{68,69} The difference in the polarizabilities of the DNA statistical segments ($\alpha_1 - \alpha_2$) along (α_1) and normal (α_2) to the DNA helix axis were determined from the equation:

$$\left(\frac{\Delta n}{g}\right)_{g \rightarrow 0} = \frac{4\pi}{45k_B T n_s} \frac{(n_s^2 - 1)^2}{n_s} (\alpha_1 - \alpha_2) \quad (3)$$

Here, Δn is the birefringence value of the DNA solution in the field of the flow velocity gradient g , η is a viscosity of solution, η_0 is the viscosity of the solvent, n_s is the refractive index of the solvent, k_B is the Boltzmann constant, and T is the absolute temperature. This equation is true for a negligible form effect, which is typical for DNA solutions with giant intrinsic optical anisotropy of the DNA coil. The $(\alpha_1 - \alpha_2)$ value is proportional to the DNA base pair optical anisotropy $\Delta\beta$ (difference in its polarizabilities along (β_1) and normal (β_2) to the DNA helix axis) and to the number of base pairs S in the DNA statistical segment: $\alpha_1 - \alpha_2 = S\Delta\beta$. The S value also determines the DNA rigidity: $S = A/l$ (l is the length of the base pair along the DNA helix). All measurements were carried out at 21 °C. The dynamic light method was used to estimate the micelle sizes in solutions with different salt concentrations for the cis- and trans-isomers of the surfactant. The correlation functions of the scattered light intensity were obtained using the PhotoCor complex (Russia). The results were processed by the DynaLS program. The hydrodynamic radius R_h of the particles was determined by the formula:

$$D_t = \frac{k_B T}{6\pi\eta R_h} \quad (4)$$

where D_t is the coefficient of translation diffusion of the particles, k_B is the Boltzmann constant, T is the absolute temperature, and η is the viscosity of the solvent.

MODEL AND SIMULATION

The five systems containing DNA, surfactant, and CoHex³⁺ or Na⁺ ions were considered. The composition of all simulated systems is given in Table 1.

Table 2. Partial Charges of the Atoms of the Head Group –CH₂–N–(CH₂–CH₃)₃ of the Azo Cation

atom	charge, e	no. of atoms
N	–0.100	1
C (–CH ₂ –)	–0.015	4
H (–CH ₂ –)	0.145	8
C (–CH ₃)	–0.180	3
H (–CH ₃)	0.060	9

The simulation box for each system contains four identical double-stranded DNA molecules. Each DNA consists of 21 base pairs d(GCCCAGCATTTCACCCAGATT) and has a total charge of $-42(e)$. Two DNA molecules are oriented parallel to each other and to one of the edges of the box, while the other two are in antiparallel orientation to them. The DNA molecules stretch from one face of a cube to another, so with periodic boundary conditions the DNA molecules become infinite and have no ends. This approach allows us to exclude the sticking of surfactant molecules to the ends of the DNA fragments, which is out of our interest.

The water molecules and 56 CoHex³⁺ were added into the simulation box with 4 DNA. This system is denoted as I in Table 1. In the other systems, the surfactant cation C₄-Azo-OC₆TEA⁺ is added. The cation C₄-Azo-OC₆TEA⁺ (Figure 1, hereinafter named Azo) contains the charged headgroup (“head”) and a hydrophobic tail with an azobenzene group. The positive charge of the headgroup is delocalized and distributed among the H atoms of the four –CH₂– groups connected to the nitrogen atom. Thus, charged atoms are located inside the headgroup and are less accessible to solvent and DNA molecules than in the previously considered^{62,63} case of surfactant cation C₄-Azo-OC₆TMA⁺ with methyl groups in the head.

In this work, the simulation of surfactant in the trans (systems II and III in Table 1)– and cis (systems IV and V)– forms was carried out. System II contains 4 DNA, 42 trans-Azo

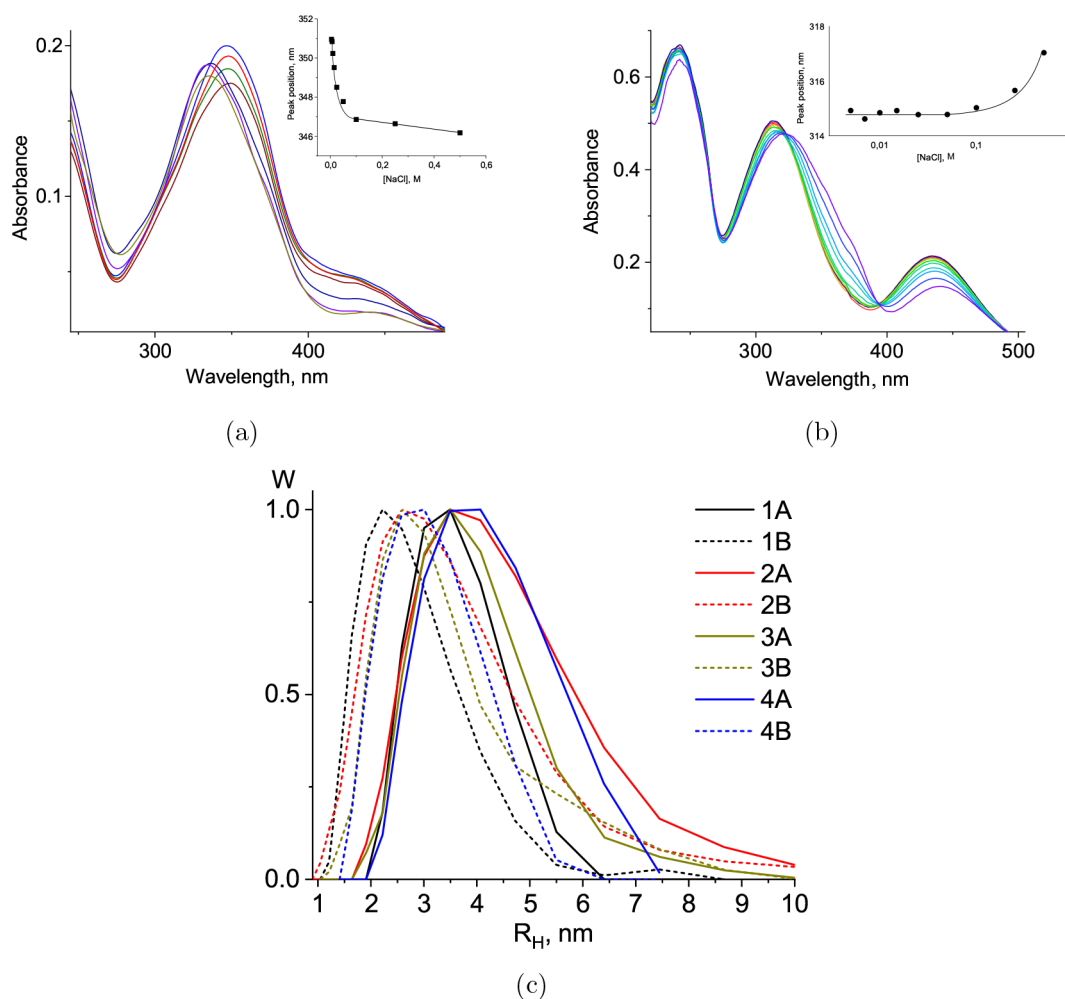


Figure 2. Effect of NaCl concentration on the absorption of (a) trans- and (b) cis-isomers of the surfactant and the size of their micelles (c). The surfactant concentration was constant: $C(\text{Azo}) = 8 \times 10^{-5}$ M (a) and 1.5×10^{-5} (b). The NaCl concentration can be determined by the insets, which indicate the peak positions for the cis- and trans-isomers at different NaCl concentrations. Part (c) demonstrates DLS data (hydration radius of micelles) for the (A) trans- and (B) cis-isomers at different ionic strengths (1, 0.005 M; 2, 0.05 M; 3, 0.15 M; and 4, 0.4 M NaCl).

cations, 42 CoHex^{3+} , and water molecules. Also, for comparison, the corresponding system containing 126 Na^+ cations instead of CoHex^{3+} is considered (system III). Systems IV and V containing cis- isomers of surfactant were obtained, respectively, from systems II and III by the trans–cis transition in Azo during 3.6 ns of simulation by slow rotation of the C–N=N–C group around its double bond by 180° .

It should be noted that, due to the fact that the volume of the simulation box is limited by computational resources, the number of CoHex^{3+} cations per DNA phosphate in the model system ($42/(21 \times 2 \times 4) = 0.25$) is higher than that in the experiments (~ 0.1).

Simulation was carried out by molecular dynamics in the AKMD program⁷⁰ using the AMBER-14sb⁷¹ force field and SPC/E model for water; compatible parameters for Na^+ developed by Dang⁷² and for CoHex^{3+} developed by Sun⁵⁶ were used. In the CoHex^{3+} model, the Co atom is bonded with $-\text{NH}_3$ groups. The charges at the atoms of the headgroup were calculated with GAMESS-16;^{73,74} see Table 2. A time step of 2 fs was used. The simulation was carried out in the NVT ensemble with a Nosé–Hoover thermostat.⁷⁵ The length of the simulation box for all of the systems was fixed to 70.98 Å, which coincides with the length of 21 base pairs of DNA. The width and height were adjusted so that the average

pressure in the system was approximately 1 atm. The temperature was kept at 25 °C. The electrostatic interactions were treated with the Ewald method.⁷⁶ The lengths of the molecular bonds were maintained with the SHAKE algorithm.⁷⁷

RESULTS OF EXPERIMENTS AND DISCUSSION

Features of DNA Interaction with the Cis- and Trans-Surfactants. Two isomeric forms of azobenzene-containing surfactant can be distinguished easily with spectroscopy. The trans-isomers predominate in aqueous solution under normal conditions (natural light, room temperature) or in the dark. The trans–cis isomerization occurs under the irradiation of the surfactant solution with UV light.

Figure 2 demonstrates spectral changes for trans-2(a) and cis-2(b) isomers of surfactant at their constant concentration $C(\text{sur})$ (in water solution $C(\text{sur}) < \text{CMC}$) with an increase in NaCl concentration, $C(\text{salt})$. Because the CMC value decreases with increasing salt concentration,⁷⁸ the observed spectral changes at high $C(\text{salt})$ reflect, among other things, the transition of the surfactants to the micellar state. Indeed, two isosbestic points for cis-isomer spectra in Figure 2b clearly demonstrate the existence of two spectral forms (before and after the formation of micelles). Note that the absence of an

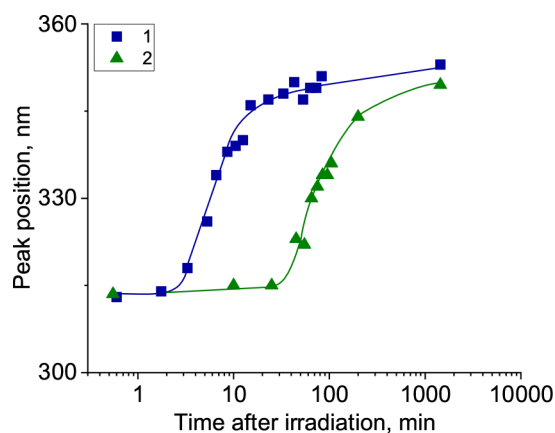


Figure 3. Change in the position of the second peak in the absorption spectra of the surfactant absorption in solutions without DNA (1) and with DNA (2) after the end of irradiation with a UV lamp.

isosbestic point in the spectra of trans-isomers with increasing $C(\text{salt})$ (Figure 2a) indicates the existence of more than two spectral forms in these systems. It is known that the emergence of micelles in surfactant solution with trans-isomers is accompanied by a blue shift of the main peak with the decrease in the intensity of the long-wavelength shoulder. Previously, we studied in detail the spectral properties of the

azobenzene-containing surfactants at different $C(\text{salt})$ values. It was shown that in the range of moderate $C(\text{salt})$ values before the CMC, alternative associates of surfactants may arise in solutions.²⁴ Thus, the spectra in Figure 2a correspond to the free trans-isomers in solution, their associates that appear at moderate $C(\text{salt})$ values, and micelles at high ionic strength. Trans–cis isomerization induces a decrease in the size of the micelles, as it was shown by the DLS method (see Figure 2c). The micelle size weakly depends on the salt concentration. It was shown that for cis-isomers the micelle size is smaller than that for trans-isomers, and the ionic strength of the solution influences it.⁶³

Because cis-isomers of surfactant can spontaneously convert over time to the trans-conformation, a special experiment determines the time interval when the properties of cis-isomers can be correctly defined (Figure 3). The change in the position of the second peak in the absorption spectra of surfactants indicates the cis–trans transition of the azobenzene group. One can see that this happens already in the third minute after irradiation of the surfactant solution with a UV lamp (at 355 nm). However, the presence of DNA slows the cis-to-trans relaxation process and guarantees a stable state of the cis-form during 10–12 min after irradiation. In the darkness, the stability of the cis-conformation increases significantly, at least to 30 min for free cis-isomers. In this regard, almost all experiments were carried out in the dark.

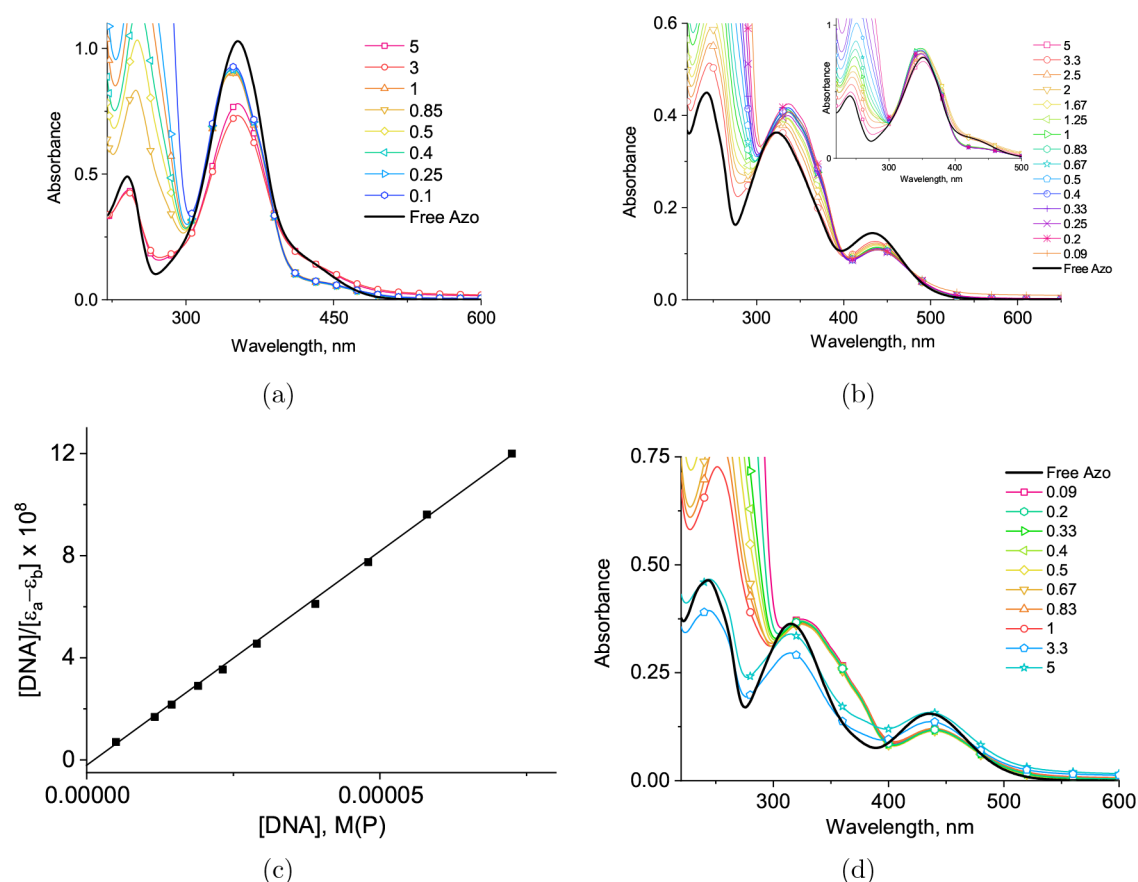


Figure 4. Results of the analysis of the absorption spectra of DNA complexes with (a) trans- and (b) cis-isomers of surfactant for different Z values (shown in the figures) in 0.005 M NaCl. The cis-isomers were mixed with DNA in solutions just before the measurements. The inset demonstrates complexes presented in (b) after irradiation with visible light (after cis–trans isomerization). The results of processing the spectra presented in (b) to determine the binding constant (the result of Wolf–Shimmer analysis of cis-isomer binding to DNA) (c). Part (d) shows the results of UV irradiation of DNA complexes with trans-isomers.

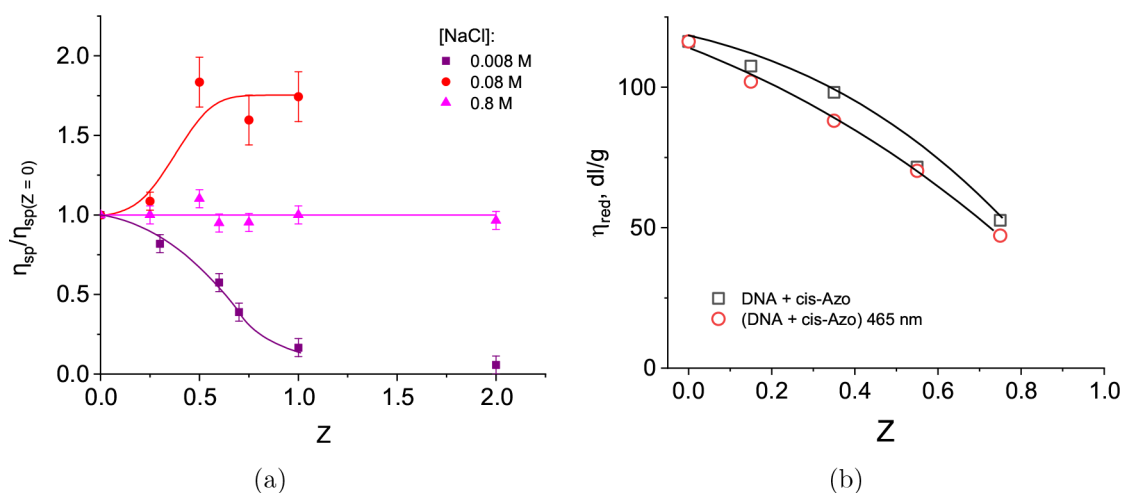


Figure 5. Dependence of the relative change in reduced viscosity of DNA solutions on the Z value for DNA–cis-isomers complexes at different NaCl concentrations (a) and the dependence of reduced viscosity of DNA–surfactant solutions in 0.005 M NaCl on Z for cis-isomers and after cis–trans isomerization of surfactant under the lighting of the same solutions at 465 nm (b); $C(\text{DNA}) = 0.007\%$.

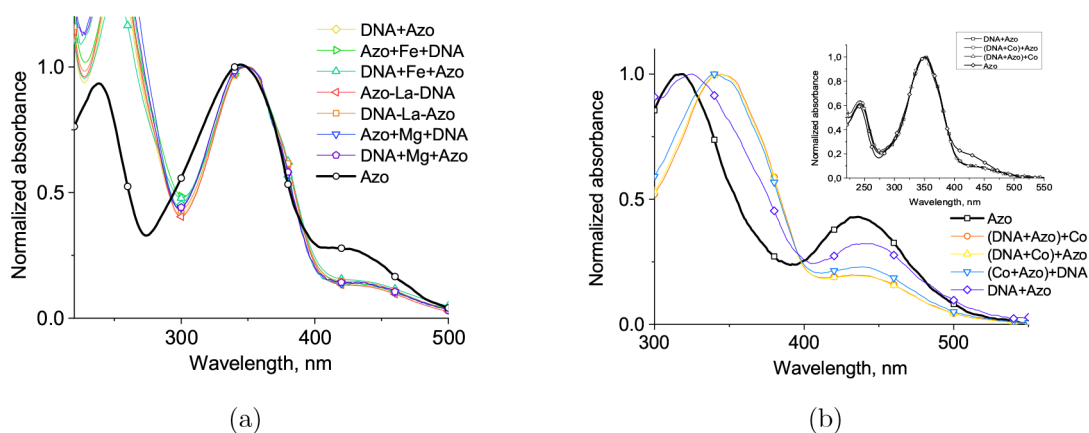


Figure 6. Normalized band maximum absorption spectra of (a) trans- and (b) cis-isomers in complexes with DNA and in the free state in 5 mM NaCl solution with and without Mg^{2+} , La^{3+} , Fe^{3+} (a) and CoHex^{3+} (b) ions in a different order of ions and surfactant adding to the DNA solution. The inset in (b) indicates DNA–trans-isomer complexes in the presence of CoHex^{3+} ; $C(\text{Azo}) = 3 \times 10^{-5}$ M, $C(\text{Mg}^{2+}) = 10^{-4}$ M, $C(\text{DNA}) = 5 \times 10^{-5}$ M, and $C(\text{La}^{3+}) = C(\text{Fe}^{3+}) = 10^{-5}$ M.

It is important for our research that trans- and cis-isomers of the surfactant interact with DNA in different ways.⁶³ The binding of trans-isomers to DNA occurs cooperatively (Figure 4a); surfactant spectra in the region of wavelengths where DNA does not absorb are clearly divided into two groups, corresponding to the free and to the DNA-bound state. Moreover, one can see the same changes in the absorption spectra of the surfactants in micelles and in complexes with DNA for all $Z < 1$ (Z is the surfactant–DNA charge ratio), even at small $Z = 0.1$. In this case, we mean the formation of “pseudomicelles” on DNA.¹³ Note that at $1 < Z < 2$, a significant deterioration in the quality of the solvent for DNA–surfactant complexes is observed, and, as a result, DNA partially precipitates. At $Z > 2$, the distinctive feature of the considered systems is the phase transition with the formation of compact homogeneous nanosized DNA–surfactant particles. Indeed, an excess of surfactant molecules in the low-concentrated DNA solution with small salt concentration induces DNA condensation.¹³ Solutions remain visually transparent. Because of the phase transition, only the absorption of molecules that are not included in complexes

with DNA is observed at $Z > 2$. The only surfactant fraction that is not involved in nanoparticles absorbs.

On the contrary, one can see a gradual change in surfactant absorption with increasing Z values for the cis-isomers (Figure 4b). The surfactant, when added to the DNA solution, was in the cis-form. The result of cis-isomers binding to DNA differs greatly from the result of UV-irradiation of DNA complexes with trans-isomers (Figure 4d). In this case, again one can see only two types of spectra for free and bound cis-isomers (like in Figure 4b for the trans-isomers). Hence, it follows that UV irradiation of the already formed DNA complexes with trans-isomers does not disturb the binding, and surfactants in complexes simply change their conformation, remaining in contact with DNA.

In Figure 4b, the smallest Z value corresponds to an excess of binding sites on DNA (high DNA concentration in the surfactant solution). There is a great difference in the spectra of the DNA-bound surfactant and of the free one. Isosbestic points demonstrate that an increase in the Z value leads to the coexistence of free and DNA-bound surfactant molecules in solution. This is a characteristic of the so-called equilibrium binding. In this case, in contrast to DNA–trans-isomer

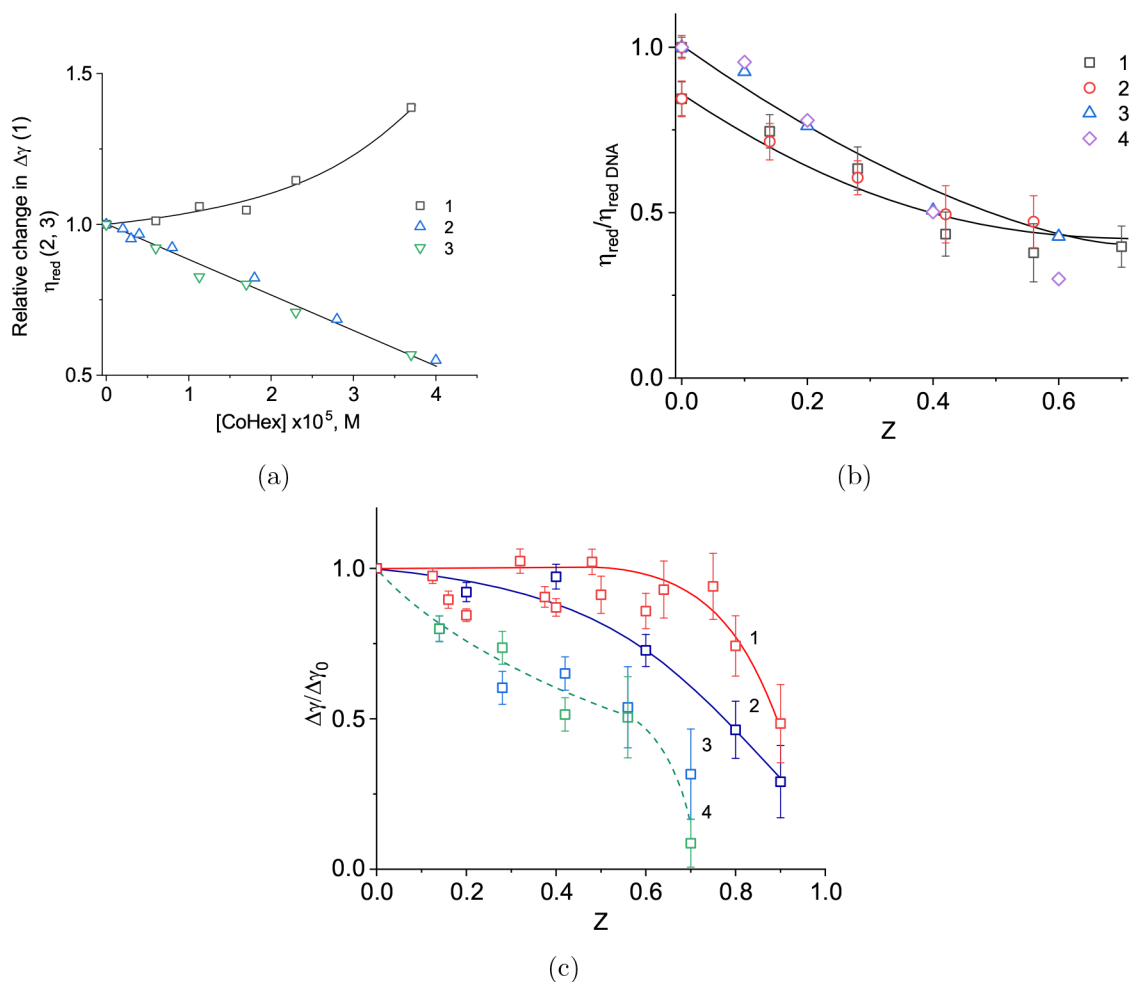


Figure 7. Influence of cobalt hexamine ions on the DNA–surfactant interaction (on the tertiary structure of DNA). Dependence of the relative change in DNA optical anisotropy $\Delta\gamma$ (1) and in the reduced viscosity of DNA solutions (2, 3) on CoHex^{3+} concentration in 5 mM NaCl (a); the dependence of the relative change in reduced viscosity (b) of DNA solutions on Z with trans- (1, 3) and cis- (2, 4) isomers with (3, 4) and without (1, 2) CoHex^{3+} , $C(\text{DNA}) = 0.007\%$ (1, 2) and 0.004% (3); $C(\text{CoHex}^{3+}) = 1.5 \times 10^{-5}$; and the dependence of the relative change in DNA optical anisotropy for the same systems (c).

systems, we can estimate the equilibrium binding constant according to the equation:⁷⁹

$$\frac{[\text{DNA}]}{|\varepsilon_a - \varepsilon_f|} = \frac{[\text{DNA}]}{|\varepsilon_b - \varepsilon_f|} + \frac{1}{K_b(|\varepsilon_b - \varepsilon_f|)} \quad (5)$$

In this equation, $[\text{DNA}]$ is the concentration of DNA in moles of base pairs, and ε_f , ε_b , and $\varepsilon_b - \varepsilon_f$ are the extinction coefficients of free, fully bound surfactant, and surfactant in the complex with DNA, respectively. K_b is the equilibrium binding constant.

Estimation of the value of the equilibrium binding constant K_b of cis-isomers to DNA gives the value of $K_b = (2 \pm 0.5) \times 10^5 \text{ M}^{-1}$. This is a fairly large binding constant. At least it is greater by an order of magnitude than that estimated for the electrostatic binding of divalent metal ions to DNA. Binding is noncooperative. From the latter, it can be concluded that for cis-isomers, the association of hydrophobic surfactant tails upon binding to DNA is not as significant as for the trans-isomers. The DNA–surfactant complex is stabilized by surfactant–surfactant intermolecular contacts for the DNA-bound molecules, which provides a stronger interaction as compared to the electrostatic binding. Indeed, as it is known, monovalent counterions (“heads” of surfactants) are unable to

form relatively long-lived complexes with DNA as compared to the rate of the bound water exchange. The energy of the electrostatic interaction of univalent counterions with DNA is approximately equal to the energy of thermal motion. Therefore, additional stabilization of DNA–surfactant complexes is obligatory. We also note that, when binding, the surfactants create a more hydrophobic environment around DNA with a lower dielectric constant, which increases the energy of the electrostatic interaction of oppositely charged ions in solution.

Effect of the Concentration of Monovalent Ions (NaCl) on the DNA–Surfactant Interaction. Without any doubt, electrostatic interactions in DNA–surfactant binding play a very important role. The polyelectrolyte swelling of the DNA coil in a solution decreases with the growth in NaCl concentration. Note that within the range of salt concentrations used in our experiments, the persistent length of DNA does not change and remains equal to $(50 \pm 5) \text{ nm}$ (the data of flow birefringence and viscosity). DNA interaction with trans-isomers of surfactant examined by viscometry has been discussed in detail earlier.¹³ Let us dwell on the analysis of DNA binding with cis-isomers. The addition of cationic surfactant into DNA solution induces different changes in

solution viscosity depending on the ionic strength (Figure 5). DNA–surfactant interaction is not observed at a high salt concentration, as it is also known from the spectral data. A drop in the solution viscosity at a low NaCl concentration during DNA binding with cis-isomers changes to an increase with the growth of the Z value at 0.08 M NaCl due to DNA aggregation. In other words, not only an increase in Z to certain values ($1 < Z < 2$) in solutions of low ionic strength, but also an increase in the ionic strength of the solution to concentrations of the order of 0.05–0.5 M NaCl at low Z , lead to the thermodynamic instability of the solutions. DNA precipitation is observed under such conditions. This is true for both surfactant isomers.

Note that the viscosity of solutions with DNA–trans-isomers is usually lower than that for the same solutions after their UV irradiation at 353 nm, which induces trans–cis isomerization.¹³ In our work, it was shown that the irradiation of DNA solutions containing cis-isomers with the light 465 nm slightly decreases the viscosity. In other words, the cis–trans transition of surfactants bonded to DNA leads to an additional shrinkage of the DNA molecular coil. This may be due to a more efficient interaction of the hydrophobic “tails” of trans-isomers associated with DNA relative to that observed for cis-isomers.

The balance of the electrostatic repulsion of identically charged DNA groups and the change in the affinity of DNA for the solvent determines the state of the solutions. Indeed, surfactants associated with DNA provide the screening of charges of phosphate groups and at the same time reduce the hydrophilicity of DNA due to the emergence of a “coat” of hydrophobic tails around its helix.

Effect of Divalent and Trivalent Metal Ions on DNA–Surfactant Binding. One can expect that divalent or trivalent counterions in solutions due to higher charges can change significantly the DNA–surfactant interaction. Indeed, divalent and trivalent ions significantly reduce the polyelectrolyte swelling of DNA as compared to the monovalent ones.³⁶ In our experiments, the NaCl concentration in all systems was constant (0.005 M). Salt MgCl_2 was used as a source of divalent counterions. It is known that Mg^{2+} ions usually bind to DNA phosphates.³⁷ The sodium ions form an ionic atmosphere around DNA without forming any stable complexes with DNA phosphates in solutions at room temperature. The charge of the divalent metal ions provides the emergence of the so-called equilibrium binding; the fractions of DNA-bound and free magnesium ions coexist in solution. Trivalent ions bind to DNA more strongly. They prefer to bind to more than one phosphate at the same time, causing the shrinkage and a kind of structuring of the DNA molecular coil.⁴⁶ It is interesting to note that DNA binding with Mg^{2+} , La^{3+} , or Fe^{3+} does not prevent further DNA–surfactant interaction (see Figure 6a).

We also used a more complex trivalent cation, cobalt hexamine. According to some reports, it can interact with DNA bases in the grooves.^{57,58} Spectral data obtained for DNA interaction with trans-isomers in the presence of CoHex^{3+} do not differ from those obtained for Fe^{3+} and La^{3+} (see inset in Figure 6b). It was shown that for cis-isomers, as well as for trans-isomers, the order in which surfactants and CoHex^{3+} were added to the DNA solution does not play any role, but premixing the surfactant with CoHex^{3+} before adding to the DNA solution leads to slightly different results. This may indicate some interaction of cis-isomers with cobalt hexamine.

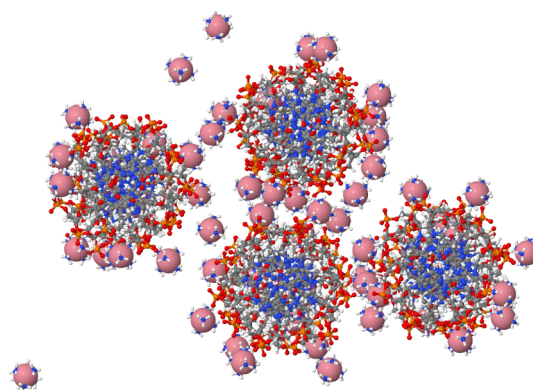


Figure 8. Condensation of DNA molecules due to CoHex^{3+} cations in system I, top view, 55 ns. The water molecules are not shown, and the cobalt of CoHex^{3+} is shown by pink spheres here and in the figures below.

Moreover, the absorption spectrum of cis-isomers upon interaction with DNA in the presence of CoHex^{3+} slightly differs from that for DNA–cis-isomer in solution without trivalent ions. Nevertheless, the spectral data indicate that the presence of CoHex^{3+} , as well as other trivalent ions, does not prevent the binding of trans- and cis-isomers of the surfactant to DNA.

It is known that Mg^{2+} and all trivalent ions used in the research prefer to bind to the DNA phosphates, which are also the main binding sites for the positive heads of surfactants. The high charge of the trivalent ions is responsible for their strong binding to DNA phosphates with the reorganization of the DNA molecular coil due to the formation of intramolecular electrostatic “linkages”. The latter leads to a stronger shrinkage of the DNA coil than is observed when polyelectrolyte swelling is completely suppressed at 1 M NaCl. In addition, this shrinkage is accompanied by the appearance of a large number of mutually oriented rigid DNA segments, which manifests itself in an increase in the optical anisotropy of the molecular coil $\Delta\gamma$ (see, for example, Figure 7a). The other trivalent ions affect similarly a change in the DNA conformation. Figure 7a also demonstrates that the DNA concentration has no influence on the measured parameters; only the concentration of the introduced cobalt ions is important and not the charge ratio, as is observed for the DNA–surfactant interaction. This difference in the DNA binding with small ions and with polycations was analyzed earlier in this Article.³⁴ Interestingly, surfactant influence on DNA polyelectrolyte swelling in this regard is similar to that for polycations, apparently due to the fact that in solutions the surfactant molecules in most cases form associates with each other.

Despite the fact that the absorption spectra of surfactants upon binding to DNA change in the same way in solutions containing di- or trivalent metal ions and without them, the DNA tertiary structure in such solutions behaves differently. Spectral data show that surfactant molecules find the opportunity to bind to DNA after the formation of DNA complexes with di- and trivalent ions. It means that not all phosphates are involved in binding to metal ions, and the overall decrease in the screening of the DNA surface charge does not play a role in this case. In contrast, in 1 M NaCl, the excess of small monovalent counterions prevents surfactant interaction with DNA via the effect on the excluded volume of DNA. Indeed, the addition of cobalt ions to the DNA–

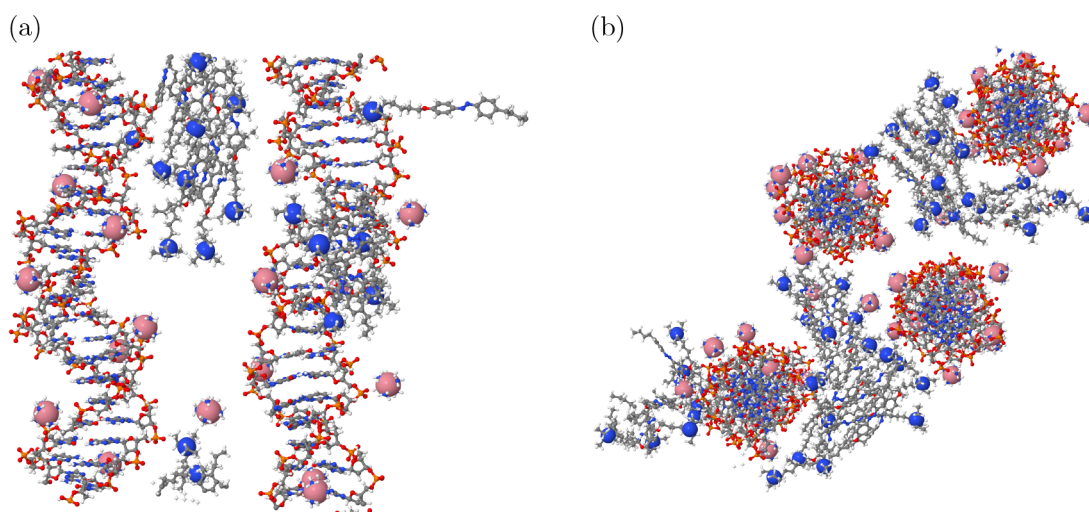


Figure 9. System II. Two DNA molecules (side view), 30 ns (a), and four DNA molecules (top view), 86 ns (b), connected by surfactant aggregates. The nitrogen atoms of the “head” of the surfactant cations are shown by blue spheres here and in the figures below.

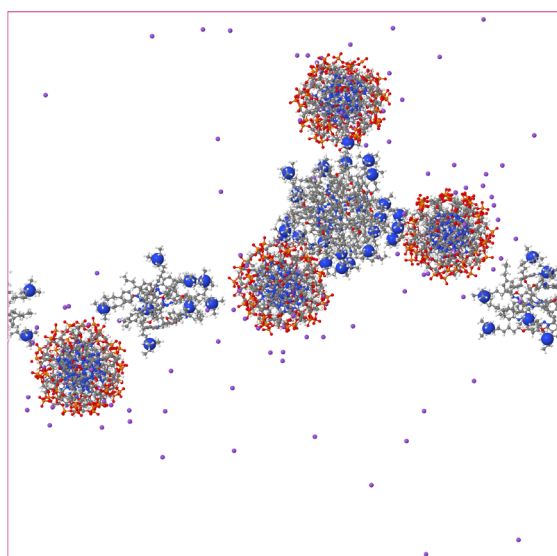


Figure 10. System III at 92 ns, top view. The Na^+ ions are shown in violet color.

surfactant solution at $Z < 0.5$, as well as the addition of the surfactant to the formed DNA–cobalt complexes, leads to an additional drop in the volume of the macromolecule up to $Z < 0.5$ when DNA is significantly compacted (Figure 7b).

Experimental measurement of the DNA optical anisotropy in solutions with a surfactant shows that neither the persistent length of DNA nor the average difference in the polarizabilities of the DNA base pairs change at under $Z < 0.8$ for the trans- and cis-isomers. Only the polyelectrolyte swelling of DNA shows a decrease. The addition of cobalt hexamine to DNA–surfactant solutions leads to a drop in the optical anisotropy of the macromolecule already at $Z > 0.1$. Accordingly, the binding of CoHex^{3+} to DNA leads to an increase in its optical anisotropy (see Figure 7a, curve 1). We can assume in this case that the persistent length of DNA decreases under these conditions. In addition, DNA packaging can be accompanied by a decrease in the asymmetry of the molecular coil (its transition to a more spherical shape is possible).

The considered data set allows us to conclude that the electrostatic interactions play a very significant role in DNA surfactant interaction indeed. First, the ionic strength of the solution, which is provided by a certain concentration of salt, has a huge impact on DNA shrinkage induced by the surfactant. It affects also the association of surfactant molecules with each other. The different type of binding of trans- and cis-isomers (cooperative for trans- and noncooperative for cis-isomers) does not influence the possibility of di- and trivalent ion association to DNA. Apparently, in both cases, the surfactant molecules are located on DNA in the form of pseudomicelles, leaving the possibility for the subsequent binding of two- or trivalent ions. However, it should be noted that the UV-induced trans–cis transition in the case of complexes formed does not lead to a destruction of DNA–surfactant complexes, but promotes the transition of DNA-bound trans-surfactant molecules to their cis-conformation. In addition, screening of the DNA charge by divalent and trivalent ions also does not prevent the subsequent binding of surfactant molecules, which find the remaining unshielded phosphate groups of the macromolecule to bind. In this case, if unshielded phosphates remain on the macromolecule, the surfactant binds to DNA according to the usual scenario (as in a NaCl solution).

To confirm the above assumptions, let us turn to the results of modeling of DNA systems with cobalt hexamine.

RESULTS OF MODELING

DNA Condensation by Cis- and Trans-Surfactants in the Presence of Cobalt Hexamine. During the first few nanoseconds, CoHex^{3+} cations in systems I, II, and IV (see Table 1) are condensed on DNA phosphates and remain there until the end of the simulation time. At the same time, surfactant cations (systems II and IV) were mostly still moving freely in the solution. Later, the surfactant cations began to aggregate with each other in solution as well as to bind to DNA phosphates and to form aggregates on DNA. The structure of the aggregates for the cis- and trans-surfactants has been studied in detail earlier.^{62,63} Obviously, small trivalent cations have an advantage over the monovalent surfactant cations in binding to DNA phosphates.

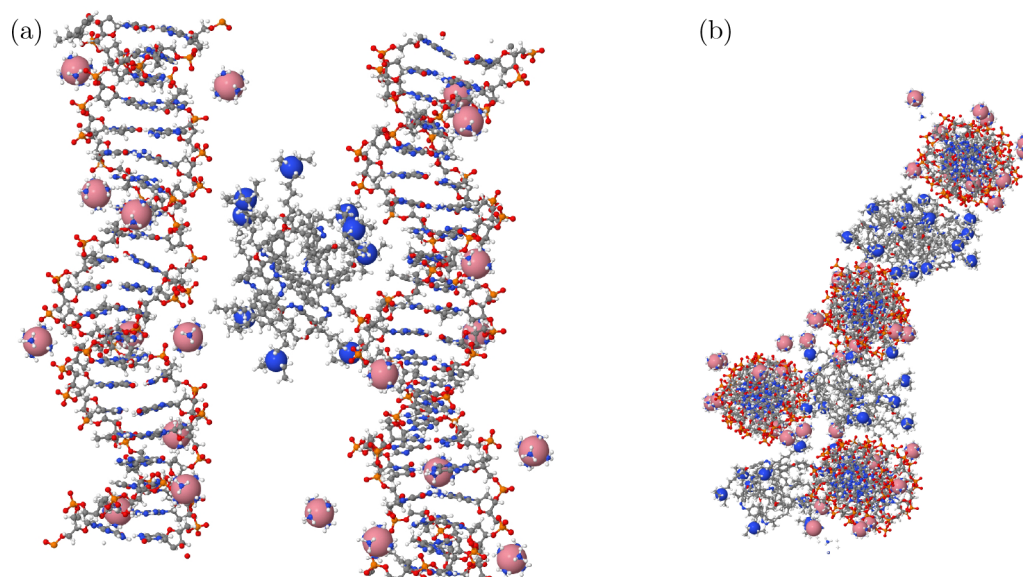


Figure 11. System IV. Two DNA molecules (side view), 31 ns (a), and four DNA molecules (top view), 82 ns (b), connected by surfactant aggregates.

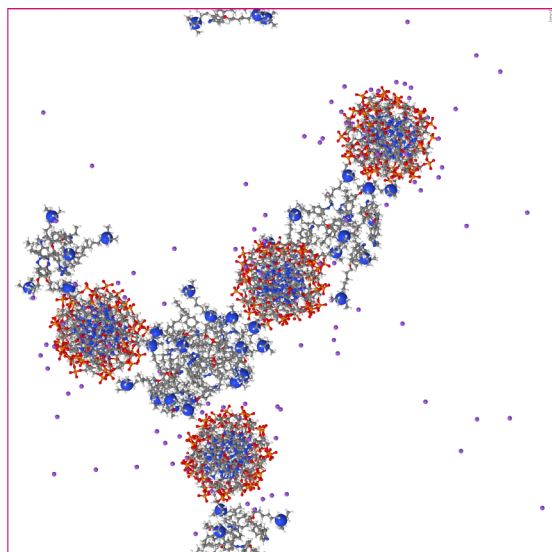


Figure 12. System V at 145 ns, top view.

In the system containing DNA and CoHex^{3+} (system I) in a time of approximately 25 ns, two DNA molecules approached each other up to a distance (between the phosphates) of approximately 1 nm. A little bit later (30 ns), the other two molecules also approached each other, and then joined together with the duplex formed before. This reflects well the experimentally observed tendency for cobalt ions to bind distant segments of the macromolecule with the formation of mutually parallel helical sections. By the end of the simulation time (55 ns), the smallest DNA–DNA spacing turned out to be approximately 0.5 nm; see Figure 8. This is in good agreement with the simulation result in the work,⁵⁶ where DNA condensation due to CoHex^{3+} cations was also observed, and the first maximum of the phosphate–phosphate radial distribution functions was about 0.7 nm.

In the system containing surfactant in the trans-form in the presence of CoHex^{3+} (system II), after about 12 ns the DNA molecule with an attached surfactant aggregate approaches

another DNA at a distance of about 2 nm; see Figure 9a. The surfactant aggregate between DNA molecules is oriented so that the surfactant cations in it are parallel to the DNA chains. Approximately at 40 ns of simulation, one more molecule joined these two DNAs, and a little later (at 50 ns) the remaining molecule joined them; the final configuration is shown in Figure 9b. In the control system (III) containing Na^+ ions, at about the same time as in the system II, two DNA molecules also approached each other, and a surfactant aggregate gradually was formed between them, linking these two molecules. As a result (at 48 ns), all four DNA molecules were connected through a surfactant cation, forming a chain (Figure 10).

The cis-surfactant cations form aggregates in solution and on DNA phosphates (systems VI and V), although not as fast as in the case of trans-surfactants. Indeed, experiments have shown that trans-surfactants, in contrast to cis-isomers, bind to DNA cooperatively. In system IV containing CoHex^{3+} , approximately 30 ns after the start of simulation, two DNA molecules stick together through a surfactant aggregate (Figure 11a), which is much later than in the case of the trans-surfactant (12 ns, system II). At 50 ns, all four DNAs stick together; the final conformation is shown in Figure 11b. In the same system with Na^+ ions (system V), DNA molecules began to stick together also approximately at 30 ns after the start of simulation too. The final conformation is shown in Figure 12; it looks like the final conformation of the system with CoHex^{3+} cations.

Binding of CoHex^{3+} Cations to DNA Base Pairs. To see the difference in the interaction of cobalt hexamine with the GC and AT base pairs, for a system containing DNA and CoHex^{3+} cations (system I), the spiral staircase distribution functions (SSDF)⁸⁰ were calculated; see Figure 13. The SSDF shows the concentration of hydrogen atoms of the CoHex^{3+} cation, averaged over all layers containing base pairs of a certain type (AT or GC) of the considered DNA fragment and over the simulation time. It is easy to see that the maximum of the concentration of CoHex^{3+} cations around the GC pair is opposite to the major groove of DNA (near N7 guanine), and that around the AT base pair is opposite to the minor groove,

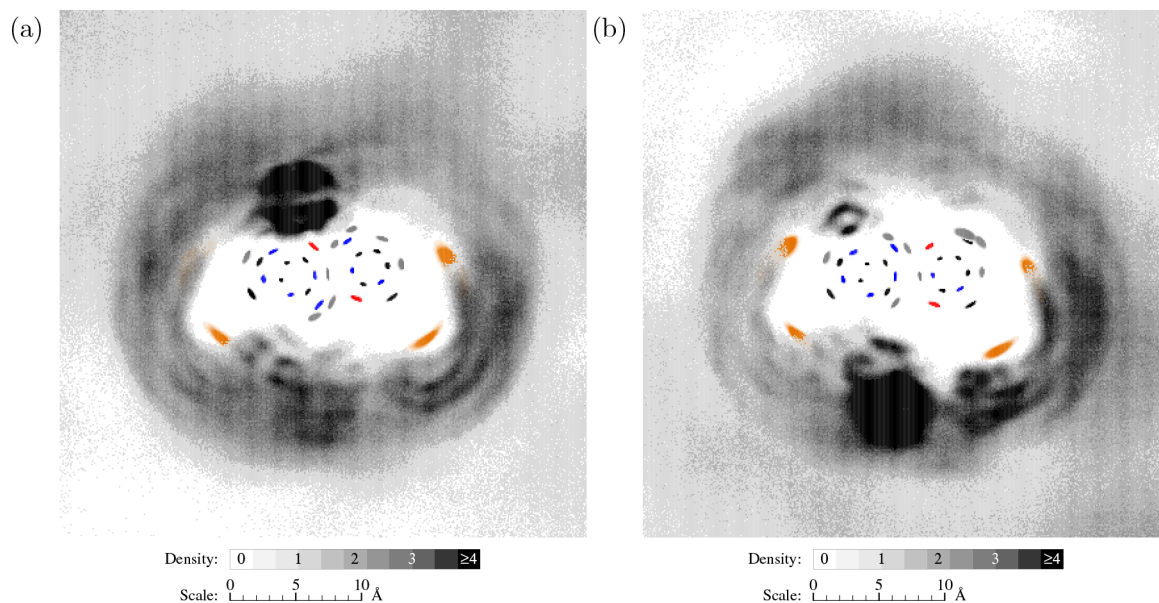


Figure 13. SSDF for the hydrogen atoms of CoHex^{3+} around the GC (a) and AT (b) DNA base pairs. DNA atoms are shown by black (C), blue (N), red (O), gray (H), and yellow (P). The value 1 on the density map corresponds to the mean density of the hydrogen atoms of CoHex^{3+} in the simulation box.

but CoHex^{3+} does not penetrate in the minor groove. These results are consistent with the simulation work⁵⁷ and the spectral experiments.⁵⁸

CoHex^{3+} cations condense on DNA and create a single-layer “coat” on DNA, in contrast to mobile monovalent Na^+ ions, which form a two-layer and extended ionic atmosphere around DNA. SSDF functions for sodium ions were obtained.⁸⁰ It can be noted that hydrogen atoms of CoHex^{3+} can approach the DNA atoms, including those in grooves, as close as Na^+ ions.

CONCLUSIONS

Experimental data with Mg^{2+} , Fe^{2+} , La^{3+} , and CoHex^{3+} and simulation with CoHex^{3+} show that the addition of di- and trivalent cations to the solution does not qualitatively change the interaction of the cis- and trans-surfactants with DNA. The binding constant for the cis-isomers was estimated. Moreover, the different type of binding of the trans- and cis-isomers (cooperative for trans- and noncooperative for cis-isomers) does not influence the possibility of di- and trivalent ion association with DNA. Apparently, in both cases, the surfactant molecules are located on DNA in the form of pseudomicelles, leaving the possibility for the subsequent binding of di- or trivalent ions. It can be noted only that CoHex^{3+} cations condense on the DNA surface faster than surfactant cations due to their larger charge and smaller size.

The association of both cis- and trans-surfactants on the surface of DNA promotes the intra- (in experiment) and intermolecular (in simulation) adhesion of DNA. Because cis-surfactant cations associate on DNA weaker than do trans-isomers, DNA condensation induced by cis-surfactant cations started later than that by trans-surfactant. This conclusion from simulation is in good agreement with the experimental data. The UV-induced trans–cis transition in the case of complexes formed does not lead to a destruction of the DNA–surfactant complexes, but promotes the transition of DNA-bound trans-surfactant molecules to their cis-conformation.

It has been observed that CoHex^{3+} is mainly attracted to DNA phosphates, but simulation also shows some weak

sequence-specific affinity toward DNA grooves. Indeed, the CoHex^{3+} ions demonstrate an attraction to the N7 atom of guanine in the major groove of DNA, but for DNA with AT base pairs CoHex^{3+} does not penetrate inside the grooves.

AUTHOR INFORMATION

Corresponding Author

Irina A. Silanteva – Faculty of Physics, Saint Petersburg University, Saint Petersburg 199034, Russia; orcid.org/0000-0002-3926-9846; Email: i.silanteva@spbu.ru

Authors

Nina A. Kasyanenko – Faculty of Physics, Saint Petersburg University, Saint Petersburg 199034, Russia

Pavel V. Gabrusenok – Faculty of Physics, Saint Petersburg University, Saint Petersburg 199034, Russia

Svetlana Santer – Experimental Physics, Institute of Physics and Astronomy, University of Potsdam, Potsdam-Golm 14476, Germany; orcid.org/0000-0002-5041-3650

Andrei V. Komolkin – Faculty of Physics, Saint Petersburg University, Saint Petersburg 199034, Russia; orcid.org/0000-0002-3577-1978

Complete contact information is available at: <https://pubs.acs.org/10.1021/acsomega.3c00419>

Notes

The authors declare no competing financial interest.

ACKNOWLEDGMENTS

Scientific research was performed at the Research park of St. Petersburg State University “Computer Center of SPbU” (<http://www.cc.spbu.ru/en>). We acknowledge Professor Pavel Vorontsov-Velyaminov from St. Petersburg University for his help in preparing this Article.

REFERENCES

- (1) Harroun, S. G.; Prévost-Tremblay, C.; Lauzon, D.; Desrosiers, A.; Wang, X.; Pedro, L.; Vallée-Bélisle, A. Programmable DNA switches and their applications. *Nanoscale* **2018**, *10*, 4607–4641.
- (2) Zhang, Y.; Zhang, Y.; Song, G.; He, Y.; Zhang, X.; Liu, Y.; Ju, H. A DNA–Azobenzene Nanopump Fueled by Upconversion Luminescence for Controllable Intracellular Drug Release. *Angew. Chem., Int. Ed.* **2019**, *58*, 18207–18211.
- (3) Morihira, K.; Hasegawa, O.; Kasahara, Y.; Mori, S.; Kasai, T.; Kuwahara, M.; Obika, S. Azobenzene-modified DNA aptamers evolved by capillary electrophoresis (CE)-SELEX method. *Bioorg. Med. Chem. Lett.* **2021**, *31*, 127607.
- (4) Zhang, L.; Liu, H.; Liu, Y.; Wu, Z. Thermodynamic stability of cis-azobenzene containing DNA materials based on van der Waals forces. *Chem. Commun.* **2022**, *58*, 3811–3814.
- (5) Kuzyk, A.; Schreiber, R.; Zhang, H.; Govorov, A. O.; Liedl, T.; Liu, N. Reconfigurable 3D plasmonic metamolecules. *Nat. Mater.* **2014**, *13*, 862–866.
- (6) Zhou, C.; Duan, X.; Liu, N. DNA-Nanotechnology-Enabled Chiral Plasmonics: From Static to Dynamic. *Acc. Chem. Res.* **2017**, *50*, 2906–2914.
- (7) Tamba, M.; Murayama, K.; Asanuma, H.; Nakakuki, T. Renewable DNA Proportional-Integral Controller with Photoresponsive Molecules. *Micromachines* **2022**, *13*, 193.
- (8) Li, J.; Wang, X.; Liang, X. Modification of Nucleic Acids by Azobenzene Derivatives and Their Applications in Biotechnology and Nanotechnology. *Chemistry – An Asian Journal* **2014**, *9*, 3344–3358.
- (9) Hiroyuki, A.; Xingguo, L.; Hidenori, N.; Daijiro, M.; Mingzhe, L.; Makoto, K. Synthesis of azobenzene-tethered DNA for reversible photo-regulation of DNA functions: hybridization and transcription. *Nat. Protoc.* **2007**, *2*, 203–212.
- (10) Bandara, H. M. D.; Burdette, S. C. Photoisomerization in different classes of azobenzene. *Chem. Soc. Rev.* **2012**, *41*, 1809–1825.
- (11) Zakrevskyy, Y.; Kopyshv, A.; Lomadze, N.; Morozova, E.; Lysyakova, L.; Kasyanenko, N.; Santer, S. DNA compaction by azobenzene-containing surfactant. *Phys. Rev. E* **2011**, *84*, 021909.
- (12) Diguët, A.; Mani, N. K.; Geoffroy, M.; Sollogoub, M.; Baigl, D. Photosensitive Surfactants with Various Hydrophobic Tail Lengths for the Photocontrol of Genomic DNA Conformation with Improved Efficiency. *Chemistry – A European Journal* **2010**, *16*, 11890–11896.
- (13) Kasyanenko, N.; Lysyakova, L.; Ramazanov, R.; Nesterenko, A.; Yaroshevich, I.; Titov, E.; Alexeev, G.; Lezov, A.; Unksov, I. Conformational and Phase Transitions in DNA–Photosensitive Surfactant Solutions: Experiment and Modeling. *Biopolymers* **2015**, *103*, 109–122.
- (14) Le Ny, A.-L. M.; Lee, C. T. Conformation and dynamics of DNA molecules during photoreversible condensation. *Biophys. Chem.* **2009**, *142*, 76–83.
- (15) Sollogoub, M.; Guieu, S.; Geoffroy, M.; Yamada, A.; Estévez-Torres, A.; Yoshikawa, K.; Baigl, D. Photocontrol of Single-Chain DNA Conformation in Cell-Mimicking Microcompartments. *ChemBioChem* **2008**, *9*, 1201–1206.
- (16) Rudiuk, S.; Yoshikawa, K.; Baigl, D. Enhancement of DNA compaction by negatively charged nanoparticles. Application to reversible photocontrol of DNA higher-order structure. *Soft Matter* **2011**, *7*, 5854–5860.
- (17) Zinchenko, A. A.; Tanahashi, M.; Murata, S. Photochemical Modulation of DNA Conformation by Organic Dications. *ChemBioChem* **2012**, *13*, 105–111.
- (18) Zakrevskyy, Y.; Titov, E.; Lomadze, N.; Santer, S. Phase Diagrams of DNA-Photosensitive Surfactant Complexes: Effect of Ionic Strength and Surfactant Structure. *J. Chem. Phys.* **2014**, *141*, 164904.
- (19) Guo, X.; Cui, B.; Li, Y.; Ding, J. Effects of salt and temperature on single-chained cationic surfactant/oligodeoxynucleotide vesicle formation. *J. Polym. Sci., Part A: Polym. Chem.* **2012**, *50*, 1740–1745.
- (20) Zhu, D.-M.; Evans, R. K. Molecular Mechanism and Thermodynamics Study of Plasmid DNA and Cationic Surfactants Interactions. *Langmuir* **2006**, *22*, 3735–3743.
- (21) Guo, Q.; Zhang, Z.; Song, Y.; Liu, S.; Gao, W.; Qiao, H.; Guo, L.; Wang, J. Investigation on interaction of DNA and several cationic surfactants with different head groups by spectroscopy, gel electrophoresis and viscosity technologies. *Chemosphere* **2017**, *168*, 599–605.
- (22) Dias, R. S.; Lindman, B.; Miguel, M. G. Interactions between DNA and surfactants. *Trends in Colloid and Interface Science XV*; Springer: Berlin, Heidelberg, 2001; pp 163–167.
- (23) Saito, T.; Iwaki, T.; Yoshikawa, K. Small Anion with Higher Valency Retards the Compaction of DNA in the Presence of Multivalent Cation. *Biophys. J.* **2009**, *96*, 1068–1075.
- (24) Kasyanenko, N.; Unksov, I.; Bakulev, V.; Santer, S. DNA Interaction with Head-to-Tail Associates of Cationic Surfactants Prevents Formation of Compact Particles. *Molecules* **2018**, *23*, 1576.
- (25) Dubin, P.; Principi, J.; Smith, B.; Fallon, M. Influence of ionic strength and composition on the size of mixed micelles of sodium dodecyl sulfate and Triton X-100. *J. Colloid Interface Sci.* **1989**, *127*, 558–565.
- (26) Maeda, H.; Muroi, S.; Kakehashi, R. Effects of Ionic Strength on the Critical Micelle Concentration and the Surface Excess of Dodecyltrimethylamine Oxide. *J. Phys. Chem. B* **1997**, *101*, 7378–7382.
- (27) Palladino, P.; Ragone, R. Ionic Strength Effects on the Critical Micellar Concentration of Ionic and Nonionic Surfactants: The Binding Model. *Langmuir* **2011**, *27*, 14065–14070.
- (28) Gunnarsson, G.; Joensson, B.; Wennerstroem, H. Surfactant association into micelles. An electrostatic approach. *J. Phys. Chem.* **1980**, *84*, 3114–3121.
- (29) Flory, P. J. *Principles of Polymer Chemistry*; Cornell University Press: Ithaca, NY, 1971.
- (30) Kasyanenko, N.; Dribinsky, B. Similarities and differences in the influence of polycations and oligomers on DNA conformation and packaging. *Int. J. Biol. Macromol.* **2016**, *86*, 216–223.
- (31) Kabanov, A. V.; Kabanov, V. A. DNA Complexes with Polycations for the Delivery of Genetic Material into Cells. *Bioconjugate Chem.* **1995**, *6*, 7–20.
- (32) Slita, A.; Kasyanenko, N.; Nazarova, O.; Gavrilo, I.; Eroplina, E.; Sirotkin, A.; Smirnova, T.; Kiselev, O.; Panarin, E. DNA-polycation complexes Effect of polycation structure on physicochemical and biological properties. *J. Biotechnol.* **2007**, *127*, 679–693.
- (33) Kasyanenko, N. A.; Zanina, A. V.; Nazarova, O. V.; Panarin, E. F. DNA Interaction with Complex Ions in Solution. *Langmuir* **1999**, *15*, 7912–7917.
- (34) Dribinskii, B. A.; Kasyanenko, N. A. Effect of the oligopeptide length on the DNA condensation process in aqueous-salt solutions. *Journal of Structural Chemistry* **2011**, *52*, 1202–1208.
- (35) Frisman, E. V.; Kas'ianenko, N. A. Hydrodynamic and optical behavior of DNA molecule in the range of high ionic strength. *Mol. Biol. (Mosk)* **1990**, *24*, 318–327.
- (36) Kasyanenko, N.; Arikainen, N.; Frisman, E. Investigation of DNA complexes with iron ions in solution. *Biophys. Chem.* **1998**, *70*, 93–100.
- (37) Granot, J.; Kearns, D. R. Interactions of DNA with divalent metal ions. III. Extent of metal binding: Experiment and theory. *Biopolymers* **1982**, *21*, 219–232.
- (38) Granot, J.; Feigon, J.; Kearns, D. R. Interactions of DNA with divalent metal ions. I. 31P-nmr studies. *Biopolymers* **1982**, *21*, 181–201.
- (39) Li, W.; Nordenskiöld, L.; Mu, Y. Sequence-Specific Mg²⁺–DNA Interactions: A Molecular Dynamics Simulation Study. *J. Phys. Chem. B* **2011**, *115*, 14713–14720.
- (40) Zhang, Z.-L.; Wu, Y.-Y.; Xi, K.; Sang, J.-P.; Tan, Z.-J. Divalent Ion-Mediated DNA-DNA Interactions: A Comparative Study of Triplex and Duplex. *Biophys. J.* **2017**, *113*, 517–528.
- (41) Tongu, C.; Kenmotsu, T.; Yoshikawa, Y.; Zinchenko, A.; Chen, N.; Yoshikawa, K. Divalent cation shrinks DNA but inhibits its compaction with trivalent cation. *J. Chem. Phys.* **2016**, *144*, 205101.
- (42) Bloomfield, V. A. DNA condensation by multivalent cations. *Biopolymers* **1997**, *44*, 269–282.

- (43) Vijayanathan, V.; Thomas, T.; Shirahata, A.; Thomas, T. J. DNA Condensation by Polyamines: A Laser Light Scattering Study of Structural Effects. *Biochemistry* **2001**, *40*, 13644–13651.
- (44) Qiu, X.; Andresen, K.; Lamb, J. S.; Kwok, L. W.; Pollack, L. Abrupt Transition from a Free, Repulsive to a Condensed, Attractive DNA Phase, Induced by Multivalent Polyamine Cations. *Phys. Rev. Lett.* **2008**, *101*, 228101.
- (45) Dias, R.; Lindman, B. E., Eds. *DNA Interactions with Polymers and Surfactants*; Wiley: Hoboken, NJ, 2008.
- (46) Kasyanenko, N.; Afanasieva, D. *DNA Self-Assembling Nanostructures Induced by Trivalent Ions and Polycations*. *Nanomaterials for Application in Medicine and Biology*; Springer: Dordrecht, 2008; pp 29–38.
- (47) Nguyen, T. T.; Rouzina, I.; Shklovskii, B. I. Reentrant condensation of DNA induced by multivalent counterions. *J. Chem. Phys.* **2000**, *112*, 2562–2568.
- (48) Besteman, K.; Van Eijk, K.; Lemay, S. Charge inversion accompanies DNA condensation by multivalent ions. *Nature Phys.* **2007**, *3*, 641–644.
- (49) Matsarskaia, O.; Roosen-Runge, F.; Schreiber, F. Multivalent ions and biomolecules: Attempting a comprehensive perspective. *ChemPhysChem* **2020**, *21*, 1742–1767.
- (50) Chien, F. T.; Lin, S. G.; Lai, P. Y.; K, C. C. Observation of two forms of conformations in the reentrant condensation of DNA. *Phys. Rev. E* **2007**, *75*, 041922.
- (51) Korolev, N.; Lyubartsev, A. P.; Rupprecht, A.; Nordenskiöld, L. Competitive substitution of hexamine cobalt(III) for Na⁺ and K⁺ ions in oriented DNA fibers. *Biopolymers* **2001**, *58*, 268–278.
- (52) Qiu, X.; Giannini, J.; Howell, S. C.; Xia, Q.; Ke, F.; Andresen, K. Ion Competition in Condensed DNA Arrays in the Attractive Regime. *Biophys. J.* **2013**, *105*, 984–992.
- (53) Deng, H.; Bloomfield, V. A. Structural Effects of Cobalt-Amine Compounds on DNA Condensation. *Biophys. J.* **1999**, *77*, 1556–1561.
- (54) Guo, Z.; Wang, Y.; Yang, A.; Yang, G. The effect of pH on charge inversion and condensation of DNA. *Soft Matter* **2016**, *12*, 6669–6674.
- (55) Todd, B. A.; Rau, D. C. Interplay of ion binding and attraction in DNA condensed by multivalent cations. *Nucleic Acids Res.* **2007**, *36*, 501–510.
- (56) Sun, T.; Mirzoev, A.; Korolev, N.; Lyubartsev, A. P.; Nordenskiöld, L. All-Atom MD Simulation of DNA Condensation Using Ab Initio Derived Force Field Parameters of Cobalt(III)-Hexamine. *J. Phys. Chem. B* **2017**, *121*, 7761–7770.
- (57) Cheatham, T. E.; Kollman, P. A. Insight into the stabilization of A-DNA by specific ion association: spontaneous B-DNA to A-DNA transitions observed in molecular dynamics simulations of d-[ACCCGCGGGT]₂ in the presence of hexaminecobalt(III). *Structure* **1997**, *5*, 1297–1311.
- (58) Ouameur, A. A.; Tajmir-Riahi, H.-A. Structural Analysis of DNA Interactions with Biogenic Polyamines and Cobalt(III)-hexamine Studied by Fourier Transform Infrared and Capillary Electrophoresis. *J. Biol. Chem.* **2004**, *279*, 42041–42054.
- (59) Wang, Y.; Ran, S.; Man, B.; Yang, G. DNA condensations on mica surfaces induced collaboratively by alcohol and hexamine cobalt. *Colloids Surf., B* **2011**, *83*, 61–68.
- (60) Santer, S. Remote control of soft nano-objects by light using azobenzene containing surfactants. *J. Phys. D: Appl. Phys.* **2018**, *51*, 013002.
- (61) Wei, J.; Liu, Y.; Chen, J.; Li, Y.; Yue, Q.; Pan, G.; Yu, Y.; Deng, Y.; Zhao, D. Azobenzene-Derived Surfactants as Phototriggered Recyclable Templates for the Synthesis of Ordered Mesoporous Silica Nanospheres. *Adv. Mater.* **2014**, *26*, 1782–1787.
- (62) Silanteva, I. A.; Komolkin, A. V.; Mamontova, V. V.; Vorontsov-Velyaminov, P. N.; Santer, S.; Kasyanenko, N. A. Some Features of Surfactant Organization in DNA Solutions at Various NaCl Concentrations. *ACS Omega* **2020**, *5*, 18234–18243.
- (63) Silanteva, I. A.; Komolkin, A. V.; Mamontova, V. V.; Gabrusenok, P. V.; Vorontsov-Velyaminov, P. N.; Santer, S.; Kasyanenko, N. A. Cis-Isomers of Photosensitive Cationic Azobenzene Surfactants in DNA Solutions at Different NaCl Concentrations: Experiment and Modeling. *J. Phys. Chem. B* **2021**, *125*, 11197–11207.
- (64) Dias, R.; Rosa, M.; Pais, A. C.; Miguel, M.; Lindman, B. DNA-Surfactant Interactions. Compaction, Condensation, Decompaction and Phase Separation. *Journal of the Chinese Chemical Society* **2004**, *51*, 447–469.
- (65) Bhattacharya, S.; Mandal, S. S. Interaction of surfactants with DNA. Role of hydrophobicity and surface charge on intercalation and DNA melting. *Biochimica et Biophysica Acta (BBA) - Biomembranes* **1997**, *1323*, 29–44.
- (66) Venancio-Marques, A.; Bergen, A.; Rossi-Gendron, C.; Rudiuk, S.; Baigl, D. Photosensitive Polyamines for High-Performance Photocontrol of DNA Higher-Order Structure. *ACS Nano* **2014**, *8*, 3654–3663.
- (67) Frisman, E. V.; Shchagina, L. V.; Vorobev, V. I. A glass rotating viscometer. *Biorheology* **1965**, *2*, 189–194.
- (68) Tsvetkov, V. N. Dynamic flow birefringence, optical anisotropy, and shape of macromolecules in solutions. *J. Polym. Sci.* **1957**, *23*, 151–166.
- (69) Cerf, R.; Scheraga, H. A. Flow Birefringence in Solutions of Macromolecules. *Chem. Rev.* **1952**, *51*, 185–261.
- (70) Komolkin, A. V.; Laaksonen, A.; Maliniak, A. Molecular Dynamics Simulation of a Nematic Liquid Crystal. *J. Chem. Phys.* **1994**, *101*, 4103–4116.
- (71) Maier, J. A.; Martinez, C.; Kasavajhala, K.; Wickstrom, L.; Hauser, K. E.; Simmerling, C. ff14SB: Improving the Accuracy of Protein Side Chain and Backbone Parameters from ff99SB. *J. Chem. Theory Comput.* **2015**, *11*, 3696–3713.
- (72) Dang, L. X. Mechanism and Thermodynamics of Ion Selectivity in Aqueous Solutions of 18-Crown-6 Ether: A Molecular Dynamics Study. *J. Am. Chem. Soc.* **1995**, *117*, 6954–6960.
- (73) Schmidt, M. W.; Baldrige, K. K.; Boatz, J. A.; Elbert, S. T.; Gordon, M. S.; Jensen, J. H.; Koseki, S.; Matsunaga, N.; Nguyen, K. A.; Su, S.; et al. General Atomic and Molecular Electronic Structure System. *J. Comput. Chem.* **1993**, *14*, 1347–1363.
- (74) Gordon, M. S.; Schmidt, M. W. In *Theory and Applications of Computational Chemistry: the First Forty Years*; Dykstra, C. E., Frenking, G., Kim, K. S., Scuseria, G. E., Eds.; Elsevier: Amsterdam, 2005; pp 1167–1189.
- (75) Hoover, W. G. Canonical Dynamics – Equilibrium Phase-Space Distributions. *Phys. Rev. A* **1985**, *31*, 1695–1697.
- (76) Ewald, P. The Calculation of Optical and Electrostatic Grid Potential. *Ann. Phys. (Berlin, Ger.)* **1921**, *64*, 253–287.
- (77) Ryckaert, J.-P.; Ciccotti, G.; Berendsen, H. J. C. Numerical Integration of the Cartesian Equations of Motion of a System with Constraints: Molecular Dynamics of n-alkanes. *J. Comput. Phys.* **1977**, *23*, 327–341.
- (78) Zakrevskyy, Y.; Roxlau, J.; Brezesinski, G.; Lomadze, N.; Santer, S. Photosensitive surfactants: Micellization and interaction with DNA. *J. Chem. Phys.* **2014**, *140*, 044906.
- (79) Wolfe, A.; Shimer, G. H. J.; Meehan, T. Polycyclic aromatic hydrocarbons physically intercalate into duplex regions of denatured DNA. *Biochemistry* **1987**, *26*, 6392–6396.
- (80) Silanteva, I.; Komolkin, A. V. Representation of DNA environment: Spiral staircase distribution function. *J. Comput. Chem.* **2018**, *39*, 2300–2306.